Available online at www.sciencedirect.com
ScienceDirect
Scripta Materialia 63 (2010) 50–53
Scripta MATERIALIA
www.elsevier.com/locate/scriptamat

Repulsive force of twin boundary on curved dislocations and its role on the yielding of twinned nanowires

Chuang Deng[a,b] and Frederic Sansoz[a,*]

[a] School of Engineering and Materials Science Program, The University of Vermont, Burlington, VT 05405, USA
[b] Department of Materials Science and Engineering, Massachusetts Institute of Technology, Cambridge, MA 02139, USA

Received 2 February 2010; revised 1 March 2010; accepted 2 March 2010
Available online 4 March 2010

The effects of twin size and sample diameter on yield stress and surface dislocation emission in twinned metal nanowires deformed uniformly were studied using classical dislocation theory and the concept of image force from twin boundaries. This theoretical study is shown to quantitatively capture the linear increase in yield stress as twin size decreases in periodically twinned Au nanowires predicted by atomistic simulations. The implication of this model as a yield criterion for realistic metal nanostructures with nanoscale growth twins is discussed.

Keywords: Nanowires; Twin grain boundary; Yield phenomena; Size effects; Dislocation theory

Predicting the yielding behavior of face-centered cubic (fcc) metal nanowires (NWs) is essential to determining the mechanical integrity of nanoscale devices. Both geometric and microstructure effects strongly influence the yield stress of fcc metal NWs under deformation [1–5]. Past experimental and theoretical studies have suggested that the process of dislocation emission from free surfaces plays a key role in size effects in nanoscale plasticity [6–9], which is fundamentally different from yielding mechanisms commonly observed in bulk metals. Equally important for the yield of metal NWs are nanoscale twins, which naturally form during synthesis [10–12], and can significantly increase the elastic limit of fcc metal nanowires in experiments [2,12]. Using molecular dynamics (MD) simulations, it has been found that coherent twin boundaries (CTBs) can act either to increase or decrease the stress required to nucleate new surface dislocations in comparison to that in twin-free NWs of corresponding diameter [13–20]. In an earlier work, we have also predicted by MD simulation that the critical resolved shear stress (CRSS) for the emission of surface dislocations in periodically twinned Au NWs, similar to that shown in Figure 1a, increases linearly with the number of CTBs per unit length [19]. In particular, such linear dependence on twin size was found more pronounced when the wire diameter decreases as shown in Figure 1b. It is therefore critically important to gain predictive understanding of the synergy between twin size and sample diameter on yield stress in twinned NWs for applications.

In this paper, using linear elastic theory, we examine the image force on a planar curved dislocation due to CTBs. We show that this model enables quantitative prediction of size effects on elastic limit in circular NWs with periodic distribution of CTBs for different values of diameter (D) and twin boundary spacing (TBS). We also discuss the implication of this image force-based model for the yield behavior of more realistic twinned nanostructures.

Chen et al. [21] have proposed an analytical model based on linear elasticity theory for the interaction of a straight screw dislocation of infinite length with a CTB in Al and Cu metals, in terms of image dislocations. In this model, the interaction is characterized by a repulsive force between the dislocation and its virtual image of negative Burgers vector with respect to the CTB given by

$$f_{CTB} = -\lambda \frac{\mu b^2}{4\pi x}, \tag{1}$$

where f_{CTB} is the force per unit length exerted by the CTB on the screw dislocation ($f_{CTB} < 0$), x is the distance between dislocation and CTB, μ is the shear modulus in the slip direction of the crystal, b is the magnitude of the Burgers vector, and λ is a dimensionless

* Corresponding author. E-mail: frederic.sansoz@uvm.edu

1359-6462/$ - see front matter © 2010 Acta Materialia Inc. Published by Elsevier Ltd. All rights reserved.
doi:10.1016/j.scriptamat.2010.03.005

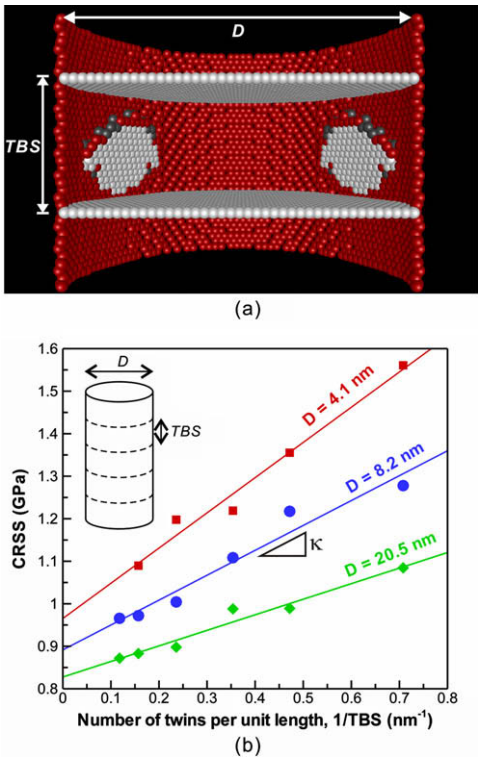

Figure 1. Molecular dynamics simulations of yielding in periodically twinned [1 1 1]-oriented Au nanowires under tensile strain. (a) Snapshot of surface dislocation emission at the junction of twin boundaries and the free surface. Atoms in white are stacking faults from twins and partial dislocations. Other non-coordinated atoms appear in red and gray. D and TBS are 12.3 and 4.2 nm, respectively. (b) Linear dependence of critical resolved shear stress ($CRSS$) on number of twin boundaries per unit length $1/TBS$ for different diameters. (For interpretation of the references to colour in this figure legend, the reader is referred to the web version of this article.)

measure of the intrinsic strength of the CTB corresponding to the elasticity mismatch between parent and twin grains in terms of shear modulus [21]. Eq. (1), however, cannot be directly used to model the interaction force between CTBs and general dislocations of arbitrary shape, which exist in realistic NWs. For example, Figure 1a shows that the yielding of twinned cylindrical NWs of Au deformed in tension with $D = 12.3$ nm and $TBS = 4.2$ nm proceeds via the nucleation of curved $\{1\,1\,1\}\langle 1\,1\,2\rangle$ Shockley dislocations at specific sites where CTBs intersect the free surface.

A representative model of surface dislocation emission on a $\{1\,1\,\bar{1}\}$ slip plane inside a twinned NW with circular cross-section is presented in Figure 2. A snapshot of the slip nucleus at the free surface obtained from atomistic simulation and its schematic illustration are shown in Figure 2a and b, respectively. These figures clearly show that the slip plane is elliptical and intersected by several CTBs separated by the same distance L_b (here $L_b = TBS/\sin\theta$ with θ the angle between the glide plane and the CTBs). It is important to note that the dislocation nucleation site is also positioned at a distance L_b from the closest CTB (Fig. 2a), because dislocation emission always occurs at the intersection between CTB and free surface [19]. In the following, we assume that the predominant interaction force acting

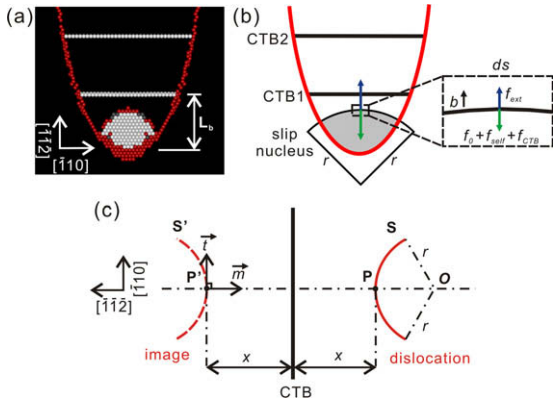

Figure 2. Model of nucleation of a curved (partial) dislocation on a $\{1\,1\,\bar{1}\}$ slip plane inside a twinned NW with circular cross-section. (a) Top view of dislocation on its elliptical glide plane from atomistic simulation and (b) its schematic illustration. The inset in (b) represents the balance of forces acting on the dislocation segment of Burgers vector $\vec{b}$, radius r and length ds. (c) Schematic of the curved dislocation (S) and its mirror image (S') across a coherent twin boundary (CTB).

on the slip nucleus is manifested by the closest CTB (CTB1 in Fig. 2b) and therefore other CTB–slip interactions are neglected.

First, let us rewrite Eq. (1) by considering the stress field of an image screw dislocation of infinite length (τ_{img}) located at a distance $2x$ away from the dislocation line ($x > 0$), such that

$$f_{CTB} = -\lambda \cdot \tau_{img} \cdot b, \tag{2}$$

with

$$\tau_{img} = \frac{\mu b}{2\pi} \cdot \frac{1}{2x}. \tag{3}$$

Eq. (3) shows that the stress field τ_{img} decreases as the distance away from the image dislocation increases. Also, any points on the image dislocation line ($x = 0$) should have a stress equal to zero due to symmetry. Therefore, it is more convenient to rewrite Eq. (3) as follows:

$$\tau_{img} = \tau(\varepsilon)\left.\frac{\varepsilon}{2x}\right|_{\varepsilon\to 0}, \tag{4}$$

with

$$\tau(\varepsilon) = \frac{\mu b}{2\pi} \cdot \frac{1}{\varepsilon}. \tag{5}$$

According to Eq. (4), the stress field τ_{img} monotonically decreases from a maximum value $\tau(\varepsilon)$ as the distance $2x$ away from the dislocation line increases (see Fig. S1 provided as Supplementary data). Here $\tau(\varepsilon)$ can be interpreted as the maximum stress at a distance $\varepsilon \sim 0$ close to the core of the image dislocation.

Likewise, we propose that the interaction force between a curved dislocation and a CTB can be calculated by considering the stress field of a curved image dislocation in the twin grain on the other side of the CTB. For that purpose, Figure 2c schematically represents a circular dislocation S of radius r and its mirror image S' with respect to the CTB. Similar to Eq. (4), the stress at point $\boldsymbol{P}$ on dislocation S due to its image S' can be expressed as

$$\tau_{img}(P) = \tau_{S'}(\varepsilon)\left.\frac{\varepsilon}{2x}\right|_{\varepsilon\to 0}, \tag{6}$$

where $\tau_{S'}(\varepsilon)$ is the maximum stress of the image dislocation S' at $\varepsilon \sim 0$ away from point $\boldsymbol{P}'$ in the principal normal direction $\vec{m}$. According to Gavazza and Barnett [22], the explicit form of $\tau_{S'}(\varepsilon)$ when $\varepsilon \to 0$ is

$$\tau_{S'}(\varepsilon) = \frac{1}{\varepsilon}\Sigma(\vec{t}) + \frac{1}{2r}\left(\Sigma(\vec{t}) + \Sigma''(\vec{t})\right)\ln\left(\frac{8r}{\varepsilon}\right) + O(1), \quad (7)$$

where $\vec{t}$ is the unit tangent to S' at $\boldsymbol{P}'$, $\Sigma(\vec{t})$ is the in-plane angular stress-factor for an infinite straight dislocation tangent to S' at point $\boldsymbol{P}'$ [23], $\Sigma''(\vec{t})$ is the second derivative of $\Sigma(\vec{t})$ with respect to $\vec{t}$. For a circular edge dislocation loop in an isotropic medium of shear modulus μ and Poisson's ratio ν [22],

$$\Sigma(\vec{t}) = \frac{\mu b}{2\pi(1-\nu)}, \quad \Sigma''(\vec{t}) = 0. \quad (8)$$

Furthermore, as depicted in the inset of Figure 2b, when the very first partial dislocation is emitted from the free surface, it is possible to assume that the applied stress (τ_{ext}) on the slip plane is equal to the critical resolved shear stress for dislocation emission (*CRSS*), such that

$$f_{ext} = \tau_{ext} \cdot b \cdot ds = CRSS \cdot b \cdot ds \quad (9)$$

and, from force equilibrium,

$$f_{ext} + f_0 + f_{self} + f_{CTB} = 0, \quad (10)$$

where f_{ext} is the external force applied on the curved dislocation segment of length ds, f_{self} and f_0 are the forces acting on ds due to line tension from the free surface, and the intrinsic energy barrier to slide two adjacent $\{1\,1\,\bar{1}\}$ planes, respectively. f_{CTB} is the repulsive force exerted by the CTB on ds. Note that in Eq. (10), we choose $f_{ext} > 0$, $f_0 < 0$, $f_{self} < 0$ and $f_{CTB} < 0$ for consistency. As shown in the inset in Figure 2b, the dislocation segment ds is pure edge with a Burgers vector $\vec{b} = \frac{1}{6}<1\,1\,2>$ as $ds \to 0$. Moreover, during dislocation nucleation it can be considered that the dislocation has not glided significantly away from the free surface. In this case, x can be approximated by

$$x \approx L_b = \frac{TBS}{\sin\theta} \quad (11)$$

with θ being the angle between the CTB and the $\{1\,1\,\bar{1}\}$ slip plane ($\theta = \cos^{-1}(\frac{1}{3})$, $b = 0.166$ nm). Therefore, the force f_{CTB} can be inferred by combining Eqs. (2), (6), (7), (8), and (11) as follows:

$$f_{CTB} = -\lambda \cdot \frac{\sin\theta}{2 \cdot TBS} \cdot \frac{\mu b}{2\pi(1-\nu)}\left\{1 + \frac{\varepsilon}{2r}\ln\left(\frac{8r}{\varepsilon}\right)\right\} \cdot b \cdot ds. \quad (12)$$

Substituting Eq. (12) into Eq. (10) and assuming minimum slip (that is, $\varepsilon = b$ [22]) allow us to determine the parameter κ, as shown in Figure 1b, which represents the dependence of *CRSS* on the number of CTBs per unit length $1/TBS$ such as:

$$\kappa = \frac{\partial CRSS}{\partial(1/TBS)} = \frac{\partial(-f_{CTB})}{\partial(1/TBS)} \cdot \frac{1}{b \cdot ds} = \lambda\frac{\mu b \sin\theta}{4\pi(1-\nu)} + \lambda\frac{\mu b^2 \sin\theta}{8\pi(1-\nu)} \cdot \frac{1}{r}\ln\left(\frac{8r}{b}\right) \quad (13)$$

Furthermore, by taking $\varepsilon = b$, it is possible to deduct the dislocation bowing radius r from the NW diameter D as follows (see Fig. S2 and mathematical derivations provided as Supplementary data).

$$r = \sqrt{\cos\theta \cdot b \cdot D}. \quad (14)$$

Eq. (14) shows that r should remain constant for the same value of D. As a result, substituting r into Eq. (13) enables us to conclude that κ should be constant, and therefore that the dependence of *CRSS* required for the emission of new surface dislocations as a function of $1/TBS$ is linear in twinned NWs of same diameter, which coincides with the linear trend shown in Figure 1b established from MD simulations.

Moreover, as mentioned above, the slope κ obtained from the fitted lines in Figure 1b increases as D decreases. In other words, the twin size-dependence of yield stress increases with decreasing NW diameter. In order to verify whether the variation of κ with respect to D agrees quantitatively with the results predicted from Eq. (13), let us write this equation as

$$\kappa = C_0 + C_1\varphi(r), \text{with } \varphi(r) = \frac{1}{r}\ln\left(\frac{8r}{b}\right), \quad (15)$$

where C_0 and C_1 are material-dependent constants. Figure 3 represents the slope κ as a function of $\varphi(r)$ for periodically twinned [1 1 1]-oriented Au NWs with a circular cross-section for D ranging from 4.2 to 24.6 nm and *TBS* from 1.4 to 8.4 nm. The plot shows a quasi-perfect linear trend of κ on $\varphi(r)$ with the coefficient of determination $R^2 = 0.99$, which strongly supports the validity of Eq. (12) to predict image dislocation effects and the repulsive force between curved dislocation and CTB.

Furthermore, it can be noted that for NWs with a diameter between 4.1 nm and 24.6 nm, the dislocation bowing radius r at the initial yield point is found to vary from 0.48 to 1.17 nm, which results in a relatively small variation in $\ln(r) = -0.74$–0.15 in comparison to $\ln\left(\frac{8}{b}\right) = 3.88$. Therefore, Eq. (15) can be approximated by a more simple expression such as

$$\kappa \approx C_0 + C_2\varphi'(r), \text{ with } \varphi'(r) = \frac{1}{r}, \quad (16)$$

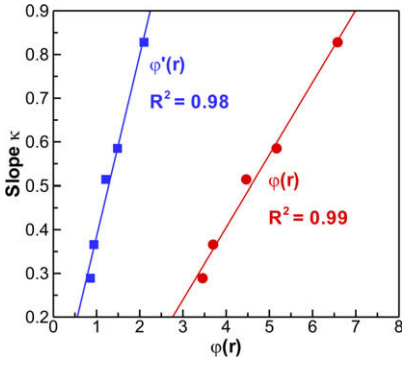

Figure 3. The change of slope κ as shown in Figure 2 for D varying from 4.2 to 24.6 nm as a function of $\varphi(r)$, with $\varphi(r) = \frac{1}{r}\ln(\frac{8r}{b})$, and $\varphi'(r) = \frac{1}{r}$. R^2 is the coefficient of determination characterizing the goodness of the linear fit.

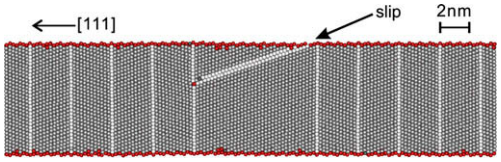

Figure 4. Onset of yielding in a gold nanowire with non-uniform distribution of twin boundaries showing surface dislocation nucleation on twin with the largest twin boundary spacing. (gray = fcc atoms, white = hcp atoms, red = surface atoms). (For interpretation of the references to colour in this figure legend, the reader is referred to the web version of this article.)

where C_2 is equal to $3.88C_1$. Figure 3 also shows that there is a good linear correlation between κ and $\varphi'(r)$ with a coefficient of determination equal to $R^2 = 0.98$, which further supports the image force-based model in characterizing the interactions between CTBs and curved dislocations. Also, Eq. (16) properly captures the increase in twin-size dependence as the diameter D, and therefore the bowing radius r, decrease.

The image force-based model presented above has three direct implications for realistic nanostructures containing nanoscale growth twins. First, this model shows that the yield stress of twinned NWs depends only on the largest CTB–dislocation distance, or largest TBS, rather than the total density of CTBs. For example, Figure 4, which represents a snapshot of MD simulation at the onset of yielding in a gold NW with non-uniform distribution of CTBs, shows that surface dislocation emission always occurs on the twin with the largest TBS. Second, a linear increase in yield stress on $1/TBS$ has also been predicted by MD simulation in periodically twinned Au NWs with faceted, zigzag surface structure [20], which proves that this model could also serve as yield criterion for different NW morphologies with nanoscale twins. For example, faceted morphologies have been observed experimentally in twinned NWs of Cu and Au [11,24]. Third, our model shows that free surfaces may also impact the yielding behavior of metallic thin films, where CTBs intersect the free surface. Therefore, caution should be exercised in interpreting dynamical dislocation emission processes from CTBs using in situ transmission electron microscopy experiments in nanotwinned thin films, similar to Ref. [25].

In summary, we have extended the image force-based model proposed by Chen et al. [21] to theoretically predict the force interactions between CTBs and curved dislocations of finite length emitted from the free surface of twinned metal NWs. It is shown that the repulsive force between CTB and a curved dislocation increases when the CTB–dislocation distance or the radius of the curved dislocation decreases. The validity of this model has been tested by successfully predicting the linear dependence of yield stress as a function of number of CTBs per unit length in periodically twinned circular Au NWs with different diameters. This theoretical study has also shown to have direct implications as yield criterion for the plastic behavior of other, more realistic nanostructures such as nanotwinned thin films and faceted NWs.

Support from the US National Science Foundation CAREER program (Grant DMR-0747658), and the computational resources of the Vermont Advanced Computing Center (NASA Grant NNX06 AC88G) are gratefully acknowledged.

Supplementary data associated with this article can be found, in the online version, at doi:10.1016/j.scriptamat.2010.03.005.

[1] B. Wu, A. Heidelberg, J.J. Boland, Nat. Mater. 4 (2005) 525.
[2] B. Wu, A. Heidelberg, J.J. Boland, Nano Lett. 6 (2006) 468.
[3] C. Ji, H.S. Park, Appl. Phys. Lett. 89 (2006) 181916.
[4] R. Dou, B. Derby, Scr. Mater. 59 (2008) 151.
[5] G. Richter, K. Hillerich, D.S. Gianola, R. Monig, O. Kraft, C.A. Volkert, Nano Lett. 9 (2009) 3048.
[6] J.R. Greer, W.D. Nix, Phys. Rev. B 73 (2006) 245410.
[7] C.A. Volkert, E.T. Lilleodden, Philos. Mag. 86 (2006) 5567.
[8] T. Zhu, J. Li, A. Samanta, A. Leach, K. Gall, Phys. Rev. Lett. 100 (2008) 025502.
[9] Z.W. Shan, R.K. Mishra, S.A. Syed Asif, O.L. Warren, A.M. Minor, Nat. Mater. 7 (2008) 115.
[10] J. Wang, M. Tian, T.E. Mallouk, M.H.W. Chan, J. Phys. Chem. B 108 (2004) 841.
[11] J. Wang, H. Huang, S.V. Kesapragada, D. Gall, Nano Lett. 5 (2005) 2505.
[12] S. Zhong, T. Koch, M. Wang, T. Scherer, S. Walheim, H. Hahn, T. Schimmel, Small 5 (2009) 2265.
[13] K. Gall, J. Diao, M.L. Dunn, Nano Lett. 4 (2004) 2431.
[14] B. Hyde, H.D. Espinosa, D. Farkas, JOM 57 (2005) 62.
[15] K.A. Afanasyev, F. Sansoz, Nano Lett. 7 (2007) 2056.
[16] A.J. Cao, Y.G. Wei, S.X. Mao, Appl. Phys. Lett. 90 (2007) 151909.
[17] Y. Zhang, H. Huang, Nano Res. Lett. 4 (2009) 1931.
[18] C. Deng, F. Sansoz, Nano Lett. 9 (2009) 1517.
[19] C. Deng, F. Sansoz, Appl. Phys. Lett. 95 (2009) 091914.
[20] C. Deng, F. Sansoz, ACS Nano 3 (2009) 3001.
[21] Z. Chen, Z. Jin, H. Gao, Phys. Rev. B 75 (2007) 212104.
[22] S.D. Gavazza, D.M. Barnett, J. Mech. Phys. Solids 24 (1976) 171.
[23] L.M. Brown, Philos. Mag. 15 (1967) 363.
[24] A. Halder, N. Ravishankar, Adv. Mater. 19 (2007) 1854.
[25] Y.B. Wang, B. Wu, M.L. Sui, Appl. Phys. Lett. 93 (2008) 041906.